



## City Research Online

### City, University of London Institutional Repository

---

**Citation:** Mujic, E., Stosic, N., Kovacevic, A. & Smith, I. K. (2016). Noise Control by Suppression of Gas Pulsation in Screw Compressors. In: Ahmed, N. (Ed.), *Advances in Noise Analysis, Mitigation and Control*. . InTech. ISBN 978-953-51-2675-1 doi: 10.5772/64795

This is the published version of the paper.

This version of the publication may differ from the final published version.

---

**Permanent repository link:** <https://openaccess.city.ac.uk/id/eprint/17762/>

**Link to published version:** <https://doi.org/10.5772/64795>

**Copyright:** City Research Online aims to make research outputs of City, University of London available to a wider audience. Copyright and Moral Rights remain with the author(s) and/or copyright holders. URLs from City Research Online may be freely distributed and linked to.

**Reuse:** Copies of full items can be used for personal research or study, educational, or not-for-profit purposes without prior permission or charge. Provided that the authors, title and full bibliographic details are credited, a hyperlink and/or URL is given for the original metadata page and the content is not changed in any way.



# Noise Control by Suppression of Gas Pulsation in Screw Compressors

Elvedin Mujić, Ahmed Kovačević, Nikola Stošić and  
Ian K. Smith

Additional information is available at the end of the chapter

## Abstract

The various sources of noise in screw compressors have been determined, the most significant of which are gas pulsations and these have been analysed extensively in this chapter. The parameters most affecting them have been identified and different simulation tools have been used to quantify their effect, together with a brief overview of the capabilities of each of them. Resulting from these studies, methods of reducing the pulsations were identified and the improvements resulting from them were predicted. Tests were then carried out on an industrial screw compressor and good agreement was obtained between the predicted and measured levels of noise reduction.

**Keywords:** screw compressor, noise, gas pulsations, rotor rattling, transmission error

## Nomenclature

$A$ : area

$h$ : specific enthalpy

$m$ : mass

$\dot{m}$  mass flow

$p$ : pressure

$\rho$ : density

$\dot{Q}$ : heat transfer

- 1  $t$ : time
- 2  $U$ : internal energy
- 3  $V$ : fluid velocity
- 4  $V$ : volume

## 5 **Subscripts:**

- 6  $dc$ : discharge chamber
- 7  $dc$ : discharge port
- 8  $in$ : inlet
- 9  $ou$ : outlet

## 10 **1. Introduction**

11 Screw compressors are widely used in a number of applications, including refrigeration and  
 12 air conditioning systems, transportation, the building industry, food processing and the  
 13 pharmaceutical industry. Their ability to operate with a variety of working fluids and in the  
 14 presence of injected liquids makes them a preferable choice to other types of compressor.

15 Over the past 30 years, these machines have been continuously improved, mainly by the  
 16 introduction of better manufacturing methods, which enabled advanced rotor profiles to be  
 17 developed. As a result, internal leakage and friction losses between the rotors have been  
 18 reduced. These and many other improvements have increased their flow capacity, reliability  
 19 and efficiency.

20 Screw compressors, however, generate a considerable level of noise during their operation,  
 21 which sometimes inhibits the scope for their use. In addition, it is becoming increasingly  
 22 difficult to satisfy new legislation that is focused on controlling noise at its source. More  
 23 detailed investigation of the causes of noise, in these machines, is therefore necessary. Once  
 24 these are identified and means of reducing their effect are found, attenuation procedures, such  
 25 as insulation and absorption, are easier to apply and can reduce noise to even lower levels.

26 Apart from the direct benefits of noise reduction, there are also indirect benefits, such as in  
 27 applications with tighter noise regulations, where less efficient types of machine can be  
 28 replaced by screw compressors, which have higher reliability and lower maintenance costs,  
 29 thereby bringing further benefits to both their operators and the environment.

30 Previous research activities have identified three different sources of noise in screw compres-  
 31 sors, namely: mechanical noise, fluid flow sources and system vibration. Mechanical sources  
 32 of noise have been thoroughly investigated by Stošić et al. [1] and Holmes [2] who proposed  
 33 methods for reducing their effects. Investigations of gas pulsations, regarded as the most



important fluid source of noise, have been published by different authors. These began in 1986 when Fujiwara and Sakurai [3] first measured gas pulsations, vibration and noise in a screw compressor. Subsequently, Koai and Soedel [4, 5], developed an acoustic model in which they analysed flow pulsations in a twin screw compressor and investigated their influence upon its performance. More recently, Sangfors [6, 7], Tanttari [8] and Huagen et al. [9] developed mathematical models for the prediction of gas pulsations in screw compressor suction and discharge chambers.

These authors explored the influence of various screw compressor parameters upon gas pulsations in the compressor suction and discharge chambers. The influence of the majority of them, which mainly affect the pressure difference between the compressor chambers, will be explained in more detail here. The investigation on gas pulsations carried by Mujić et al. [10] included the influence of the discharge port shape and area, as other important parameters, previously neglected.

In the present study, the effects of the different influential parameters were evaluated by the use of three different simulation models. A chamber model, which describes the screw compressor working cycle, was developed using MATLAB/SIMULINK. The model is very fast but not capable of predicting higher harmonics accurately. To improve on this, an existing full three-dimensional (3D) CFD model of flow within a screw compressor, and its discharge system, was applied. This model greatly improved the overall accuracy but was too time consuming. As a compromise a third model was developed that combined the best features of the first two. Predictions made with it were obtained in far less computational time with little difference from those obtained from the 3D CFD model, which agreed well with experimental measurements.

The results of the analyses showed that, although many parameters influence the level of gas pulsations, there are no practical means of altering most of them. However, changes in the shape of the compressor discharge port can have a strong effect and can reduce noise, even on existing machines, as was confirmed by tests. For certain working conditions such alterations can cause a minor loss in performance, but, in other cases, they can even lead to improvements.

## 2. Working principle of screw compressor

Screw compressor operation is based on volumetric changes in all three dimensions. As shown in **Figure 1**, the compressor consists, essentially, of a pair of meshing helical lobed rotors contained in a casing. The flutes formed between the lobes on each rotor form a series of working chambers in which gas or vapour is contained. Beginning at the top and in front of the rotors, shown on the left, there is a starting point for each chamber where the trapped volume is initially zero. As rotation proceeds in the direction of the arrows, the volume of that chamber increases as the line of contact, between the rotor with convex lobes, known as the male rotor and the adjacent lobe of the female rotor, advances along the axis of the rotors towards the rear. On completion of one revolution, i.e. 360° of the male rotor, the volume of the chamber reaches its maximum and extends, in helical form, along virtually the entire length of the rotor. Further rotation then leads to re-engagement of the male lobe with the succeeding

- 1 female lobe along a line of contact, starting at the bottom and front of the rotors and advancing
- 2 to the rear, as shown on the right. Thus, the trapped volume starts to decrease. On completion
- 3 of a further  $360^\circ$  of rotation by the male rotor, the trapped volume returns to zero.

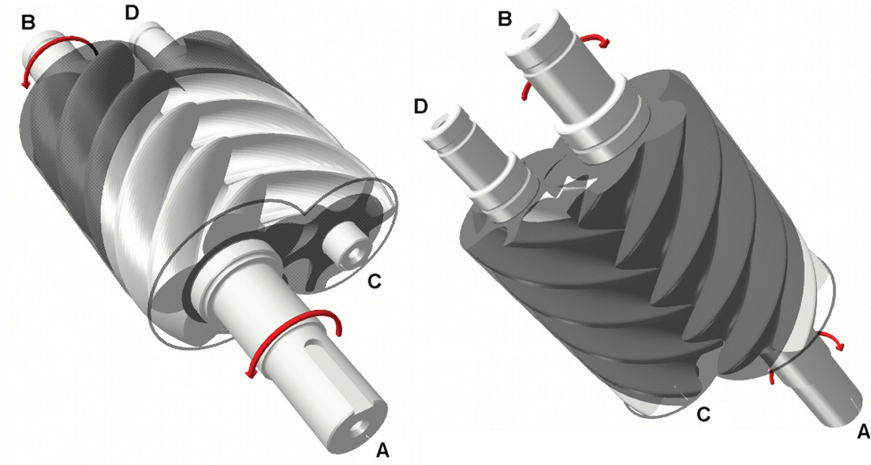


Figure 1. Working principle of a screw compressor.

AQ4

The dark shaded portions show the enclosed region where the rotors are surrounded by the casing, which fits closely round them, while the light shaded areas show the regions of the rotors, which are exposed to external pressure. Thus, the large light shaded area on the left corresponds to the low pressure port while the small light shaded region between the shaft between ends B and D on the right corresponds to the high pressure port.

Exposure of the space between the rotor lobes to the suction port, as their front ends pass across it, allows the gas to fill the passages formed between them and the casing until the trapped volume is a maximum. Further rotation then leads to cut-off of the chamber from the port and progressive reduction in the trapped volume. This continues until the rear ends of the passages between the rotors are exposed to the high pressure discharge port. The gas is then expelled through this at approximately constant pressure as the trapped volume returns to zero.

### 3. Sources of noise within a screw compressor

During the compressor operating cycle, part of the energy is dissipated in the form of flow and mechanical disturbances such as gas pulsations or rotor rattling. These generate both system vibrations and pressure waves, with a range of frequencies and intensity levels, called noise. It is impossible to remove these noise sources completely, but some improvements are possible if efforts are directed towards the reduction of the disturbances created during the compressor working process. To do that, one has to first distinguish between the different mechanisms of

noise generation and to classify them according to both, their significance and the possibility of their reduction.

### 3.1. Mechanical sources of noise

The main source of mechanical noise is intermittent contact between the compressor rotors. This is the result of variation in the torque transferred from the male to the female rotor. New and more efficient rotor profiles introduce a very small negative torque to the female rotor compared with that of the male rotor. This torque, generated by the pressure-induced forces acting on the female rotor, is of the same order of magnitude as that created by other means, such as contact friction and oil drag forces. Since the negative female rotor torque acts in the opposite direction to the other two, the net torque may change in sign from negative to positive within one lobe rotation cycle as indicated by Stošić et al. [1]. This may cause instability in the female rotor rotational motion, resulting in flutter and, in the extreme case, rattling. Stošić et al. [1] proposed a new type of “silent” profile, which maintains positive torque on the female rotor and prevents this kind of noise from occurring.

Holmes [2] suggests another reason for noise generation, called transmission error. Transmission error occurs in the driven component of a screw pair when its instantaneous angular position differs from the theoretical angular position. This causes, earlier or later than expected, contact between rotor lobes and generates noise. Holmes suggests the reasons for the existence of the transmission error might be lead mismatch, lead non-linearity, pitch errors, housing bore imperfection, bearing deflections and rotor deflection due to the gas forces. Holmes suggests relieving the rotor’s profiles to enable smoother contact between the lobes and reduce noise.

The noise reduction procedures proposed by both resulted in reported overall noise attenuation of 4–6 dBA.

### 3.2. Fluid sources of noise

According to Sangfors [6, 7], Koai and Soedel [4, 5], Tanttari [8] and Huagen et al. [9], gas pulsations are the main source of noise generated by fluid flow in screw compressors. These are created by unsteady fluid flow through the suction and the discharge ports which change the pressure within the suction and discharge chambers. The flow rate depends mainly on the pressure difference between the chambers and starts with the exposure and finishes with the cut-off of the suction or discharge port, as the rotors revolve past them.

A typical frequency spectrum of pressure pulsations in the suction and discharge chambers of the test screw compressor used in this investigation is shown in **Figure 2**. As can be seen, the gas pulsations are higher in the discharge chamber than in the suction chamber. However, while the discharge port is completely enclosed in its housing, the suction port may be more exposed to its surroundings, which are separated from the atmosphere only by the suction filter. Therefore, despite the smaller pulsations, noise generated in the suction chamber should require similar attention to that generated in the discharge chamber.

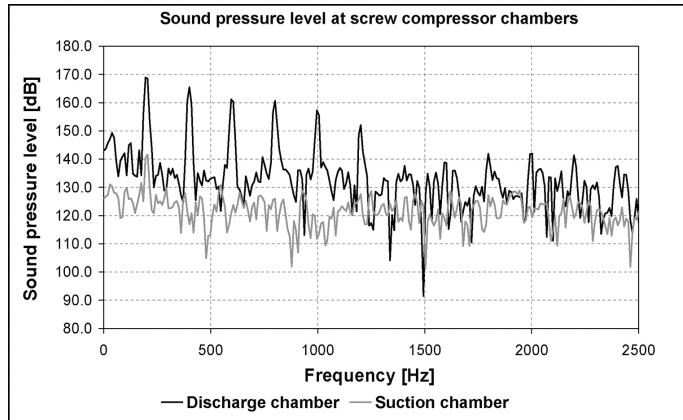


**Figure 2.** Sound pressure spectrum in suction and discharge chambers.

Another cause of fluid flow noise in screw compressors is turbulent fluid flow through the ports and the clearance gaps. Soedel [11] believes that turbulent noise contributes to the overall sound mainly in the higher frequency ranges between 3 and 6 kHz. However, compressor noise in that frequency spectrum is relatively low. So, this source of noise may be neglected.

## 4. Mathematical modelling of the discharge flow process

As mentioned in the introduction, three models for predicting flow properties within a screw compressor were applied to investigate the influence of the operational parameters and the compressor geometry upon gas pulsations. The first is a thermodynamic chamber model of the processes within a screw compressor, as described by Stošić et al. [12]. The second is a 3D CFD model which calculates the details of the fluid flow within a screw compressor, as given by Kovačević et al. [13]. As will be shown, both models are able to identify the influence of both operation and design parameters upon gas pulsations. However, the 1D model is insufficiently accurate while the 3D model requires excessive computational time.

Third, coupled simulation model was therefore employed to overcome the limitations of the first two. The new model provides a reasonably accurate result without the need for substantial computational time.

### 4.1. Mathematical model of screw compressor thermodynamics

Thermodynamic models of screw compressor performance [4, 6] have been proved to be useful tools for evaluating the influence of some of the design and operating parameters on gas pulsations in the discharge chamber. The one presented here is based on existing models described in [12, 14]. These were primarily developed to investigate the thermodynamic characteristics of a screw compressor within one working cycle. Starting from there, these

- 1 models are able to calculate screw compressor integral parameters such as mass flow rate,  
 2 compressor power, volumetric and adiabatic efficiency, etc. An updated model proposed by  
 3 Mujić et al. [10] is able to account for changes in the geometry of the port shapes.

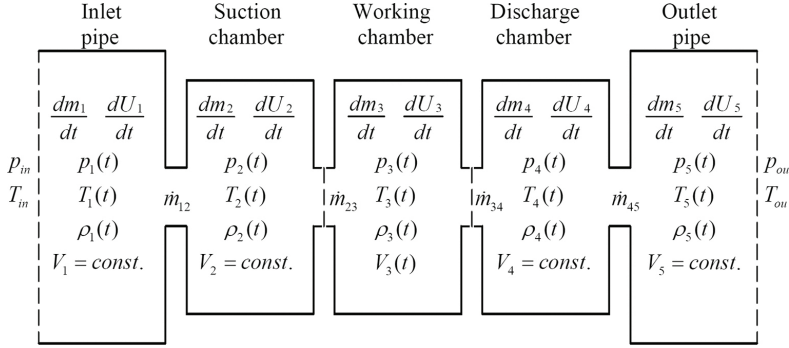


Figure 3. Thermodynamic simulation model of a screw compressor.

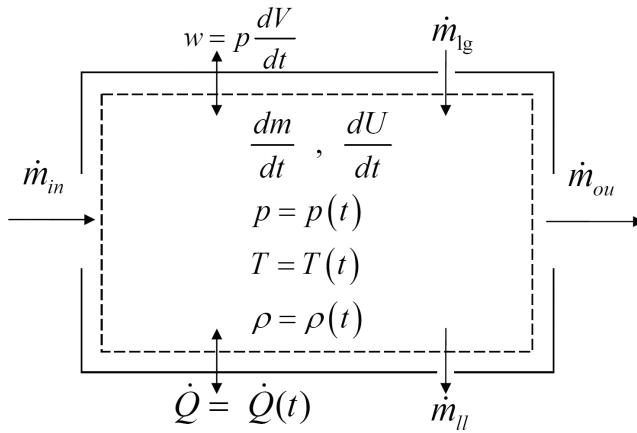


Figure 4. Screw compressor control volume for one-dimensional analysis.

Since the mathematical basis of the model used here has already been well publicised, it will be presented in a very compact form, together with results obtained from it compared with those derived from experimental tests.

As shown in Figure 3, the thermodynamic model of a screw compressor is based on the assumption of five separate control volumes. The working chamber is periodically connected to the suction and discharge chambers through flow areas, which vary with time both in shape and size. The working chamber can be also connected to neighbouring chambers through clearances during the phases of the compressor cycle when the suction and discharge ports

are closed. Other chambers are permanently connected to each other through openings of constant size throughout the working cycle.

The model assumes that all thermodynamic values, such as pressure, temperature and density, are uniform within these control volumes. Any one of these control volumes can be considered as an open thermodynamic system, which exchanges fluid mass and energy with the environment, as shown in **Figure 4**. The mass and energy flowing in and out of any control volume affect the mass and energy level of the fluid trapped inside it.

The equation of mass conservation, which describes mass variation in the control volume, is given in Eq. (1):

$$\frac{dm}{dt} = \dot{m}_{in} - \dot{m}_{ou} \quad (1)$$

This equation is common for all the control volumes within the thermodynamic model. The mass inflow into the control volume consists of the suction flow from the previous control volume, the flow of injected fluid and the leakage flow which enters the control volume. The mass outflow from the control volume is obtained from its discharge flow and the leakage flow that leaves the chamber.

The equation for conservation of internal energy within the control volume may then be written as follows:

$$\frac{dU}{dt} = \dot{m}_{in} h_{in} - \dot{m}_{ou} h_{ou} + \dot{Q} - p \frac{dV}{dt} \quad (2)$$

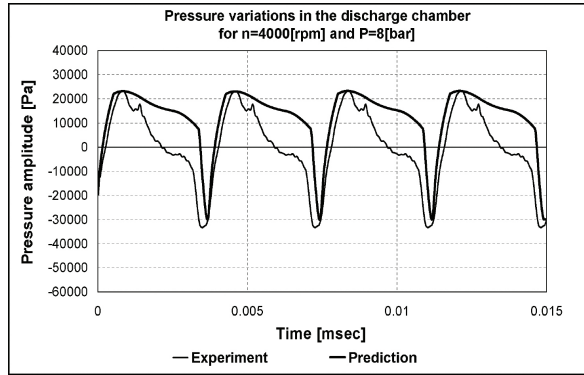
The rate of change of internal energy within the control volume is equal to the difference of energy fluxes, which the control volume exchanges with its surroundings, together with the heat transfer through the control volume boundaries and the thermodynamic work.

Other phenomena within the control volume and at its boundaries are modelled by a number of algebraic equations, which describe leakage, inlet and outlet fluid velocities, oil injection and similar effects, and the differential kinematic relations which describe the instantaneous operating volume and how it changes with rotational angle or with time. The model also includes a thermodynamic equation of state of the fluid, required to complete and close the equation set.

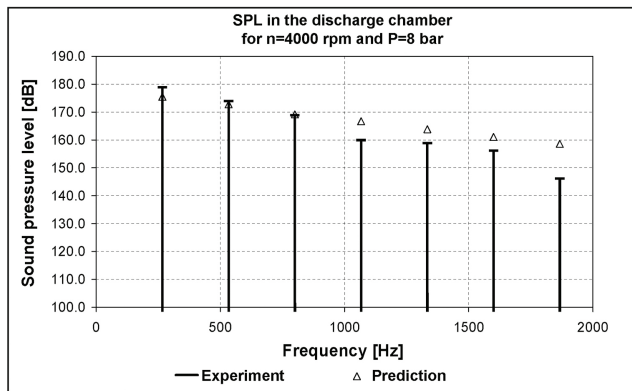
#### 4.1.1. Comparison of calculated and experimental results

The pressure history predicted by the thermodynamic model is shown for one of many sets of results in **Figure 5**. The predictions and measurements cover a set of points obtained for an

- 1 industrial screw compressor at operational speeds in the 2000–6000 rpm and discharge  
 2 pressures in the range of 5–12 bar.



3  
 4 **Figure 5.** Gas pulsations calculated by 1D model, time domain.



5  
 6 **Figure 6.** Gas pulsations calculated by 1D model, frequency domain.

7 These show that this thermodynamic model accounts very well for changes in the outlet  
 8 pressure, which affect gas pulsations significantly. The model also takes into account variation  
 9 of the shaft rotational speed and other compressor operational and geometrical parameters as,  
 10 for example, changes in the discharge port geometry. The computation time is measured in  
 11 seconds, when this model is employed. This makes it very useful for the analysis of the  
 12 influence of any of the above-mentioned parameters on the level of the gas pulsations in the  
 13 discharge chamber.

14 Although the results show that the predicted values of gas pulsations in the discharge chamber  
 15 are in line with the amplitudes corresponding to the compressor fundamental frequency and



its first harmonic, as is shown in **Figure 6**, this model does not predict higher harmonics accurately. This confirms that chamber, or even 1D, models are accurate only for a very narrow frequency range [5]. When averaged, for the amplitudes of the fundamental frequency and its first five harmonics, the prediction is from 40% to 65% in error. This value varies for different working conditions and increases for the higher harmonics.

Koai and Soedel [5], who used a finite element method, showed that it is possible to achieve better agreement using a 3D model, which accounts for the complex geometry of the compressor discharge port and chamber.

#### 4.2. Full 3D CFD model of a screw compressor

The 3D-CFD grid generation model, established by Kovačević et al. [13], was used to enable predictions of fluid flow in screw compressors to be made by means of commercial solvers Comet, StarCD or CFX. Pressure fluctuations in the compressor ports, including gas pulsations in the discharge chamber, were thus obtained, including fluid-solid interactions. Also, changes in the compressor geometry could be accounted for by means of a CAD interface.

Following recommendations expressed in [5], this model captured the higher harmonics more accurately.

##### 4.2.1. Numerical grid of the screw compressor

To apply the calculation procedure, the compressor fluid domain is replaced by a numerical grid. The compressor fluid domain is divided into different fluid domains as shown in **Figure 7**. The grid consists of both moving and stationary parts.

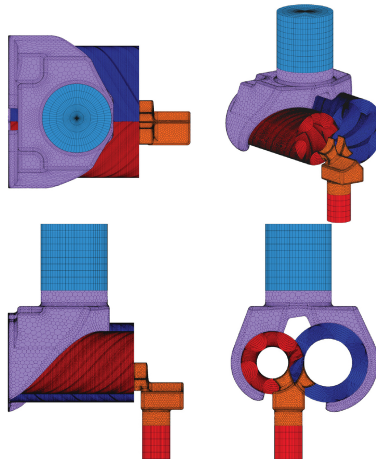


**Figure 7.** Numerical grid of screw compressor domains.



The numerical mesh of the moving rotors is produced by a specially developed grid generator for screw compressor rotor domains, as described in more detail by Kovačević et al. [13]. The same grid generator may also be used for grid generation of stationary parts of the numerical grid, such as idealised suction and discharge domains. These stationary domains can also be mapped using a commercial grid generator, for example, the one included in Star CCM+, as shown in **Figure 7**. The generated rotor grid is fully structured while stationary chambers can generally be unstructured and may consist of tetrahedral, hexahedral or polyhedral grid elements, as shown in **Figure 7**. The relatively simple domains of the inlet and outlet pipes have been discretized with hexahedral grid elements. Once generated, the sub-domains are connected over coinciding boundary regions.

#### 4.2.2. Comparison of calculated and measured results

The numerical grid of the compressor fluid domain consisted of 652,017 grid elements. One discharge process was discretized through 50 time steps. Thus, according to the compressor speed, the size of the time step was in the range of 50–150  $\mu\text{s}$ . The convergence criterion inside one time step was satisfied when residuals dropped by three orders of magnitude.

The gas pulsations predicted by the 3D model are shown in **Figure 8**, compared with the same set of measurements used for comparison with the thermodynamic model.

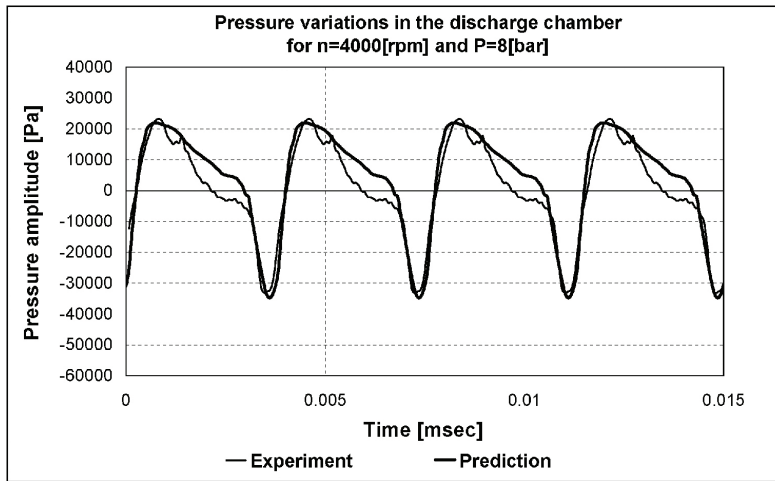


**Figure 8.** Gas pulsations calculated by 3D model, time domain.

As expected, the results presented in the frequency spectra, in **Figure 9**, show an improvement over those obtained from the thermodynamic model presented in **Figure 6**. This improvement is mainly due to enhanced prediction of the higher harmonics by including the pressure history within the discharge chamber, while taking account of the discharge chamber geometry.

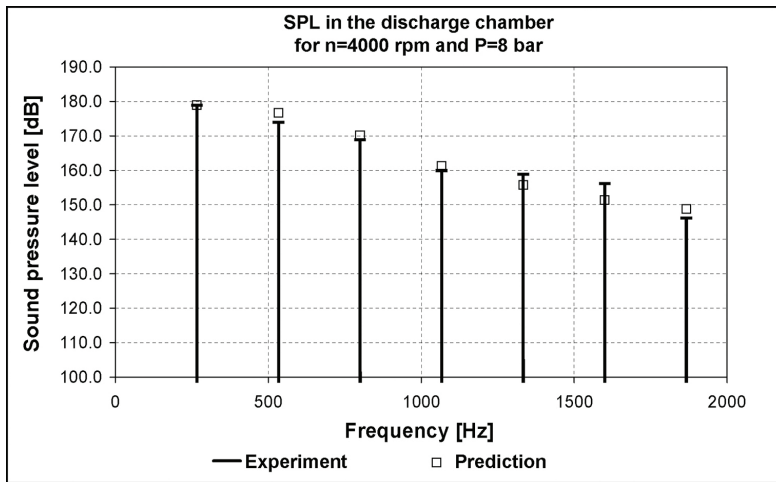


**Figure 9.** Gas pulsations calculated by 3D model, frequency domain.

The 3D model estimates non-uniform distribution of the pressure and other flow properties across the control volume, which creates pressure waves that affect the measurements.

Although the 3D model provided more accurate results, the time required for calculation was much longer than that for the thermodynamic model. The calculation of this case required between 24 and 30 hours on a PC with a 2.8 GHz Intel Xeon Dual Core processor and 2.5 GB RAM. Therefore, the evaluation of a number of different influential parameters could take weeks or even months. A new simulation model was therefore proposed to preserve the accuracy of the 3D model while reducing the calculation time.

### 4.3. Coupled model

The use of coupled models which combine a thermodynamic chamber model with a 3D model has been proposed to estimate pressure and flow changes in IC engine systems [15]. In such models, components of the system of secondary concern are simulated with a thermodynamic model and coupled with full 3D simulations for components of greater interest.

These coupled models combine the advantages of the fast computation and high flexibility of the thermodynamic model, with the enhanced capabilities of the 3D model. This permits more extensive investigation of the flow field, multiphase flow computation and chemical reactions within the cylinders.

A similar approach can be used to evaluate how the compressor operational parameters and its geometry influence gas pulsations. Therefore, a new coupled model was developed to take advantage of the 3D model while, at the same time, reducing computational time [16].

The main objects of interest are the geometrical shapes of the discharge chamber and the discharge port, both of which are in the fluid domain within the discharge chamber. The gas

flow through them was therefore simulated by a 3D model. However, the other domains of the compressor, which were of secondary interest for this purpose, were analysed with sufficient accuracy by the thermodynamic model, already described in Section 4.1. The structure of the coupled model is shown in **Figure 10**.

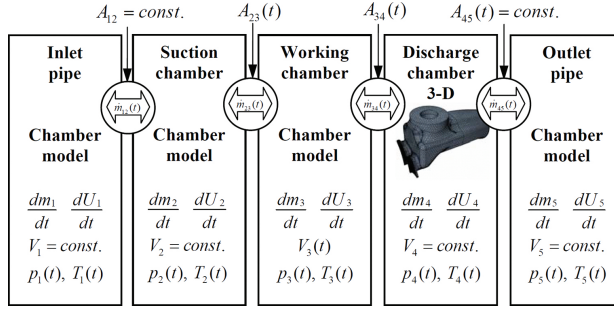


**Figure 10.** Structure of the coupled model.

The 3D CFD model of the discharge chamber is simpler than the previously described 3D model because it does not contain any moving parts. This excludes the equation of space conservation from the calculation. The numerical mesh of the discharge chambers is shown in **Figure 11**.

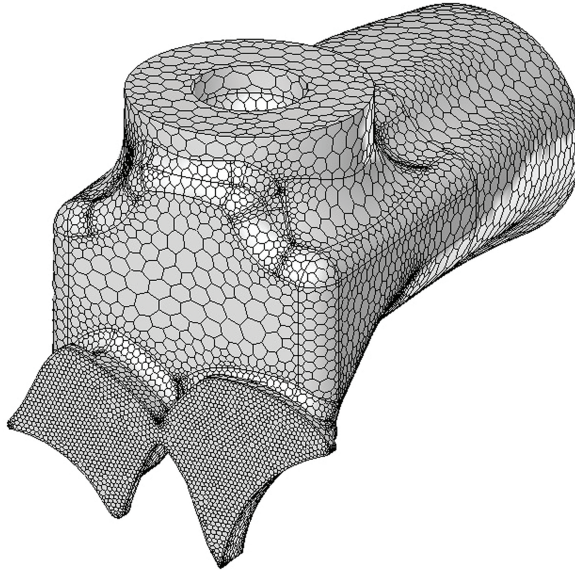
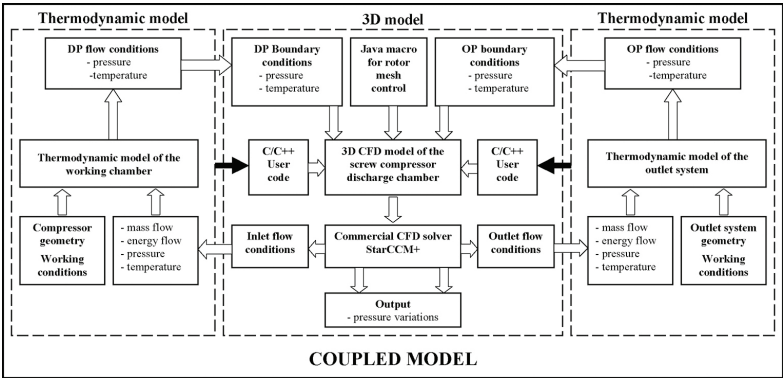


**Figure 11.** Numerical grid of the discharge chamber.

1 A commercial CFD solver Star CCM+ was used to estimate the fluid flow in the discharge  
2 chamber. The thermodynamic model, used to simulate the remaining fluid domains, was  
3 programmed as a set of user sub-routines in the CFD code. The 1D model, defined, sets the  
4 boundary conditions applied at the discharge port and the outlet of the discharge chamber for  
5 the 3D model as is shown in **Figure 12**.



7 **Figure 12.** Coupling of thermodynamic chamber model and 3D model.

8 The arrangement shown in **Figure 12** enables a full two-way coupling of the models. The  
9 pressure and temperature calculated inside the working chamber and the outlet reservoir are  
10 used as the boundary conditions passed through the interface to the 3D model, where the flow  
11 field in the discharge chamber is calculated. The pressure and velocity values on the bounda-  
12 ries are then used to integrate the boundary mass flows, which are then used to calculate new  
13 values in the chamber model. This cycle is repeated until a converged solution is obtained, in  
14 which the mass and energy flows, pressures, velocities and densities are in balance. Once  
15 converged, the next time step is initiated with the new values of the chamber volume and the  
16 flow area and the procedure is repeated.

17 *4.3.1. Comparison of calculated and experimental results*

18 The numerical grid of the compressor fluid domain consisted of 86,000 grid elements. One  
19 discharge process was discretized through 90 time steps which represents a male rotor rotation  
20 of 1 degree per time step. Depending on the compressor speed, the length of the time step was  
21 in the range of 28–83  $\mu$ s. The convergence criterion inside one time step was satisfied when  
22 the residuals dropped by three orders of magnitude. As for the full three-dimensional method,  
23 calculation of four cycles of the discharge process was necessary to obtain a convergent  
24 solution.

25 The coupled model was validated by use of the same set of experimental data as for the  
26 thermodynamic and 3D models. Examples of the results calculated by the coupled model are  
27 shown in **Figures 13** and **14**. These results show far better prediction of the gas pulsations in

the discharge chamber than those obtained from the thermodynamic model, at one position in the computational domain. As can be seen, these are almost identical with those obtained from the 3D model. The coupled model predicts pulsation amplitudes for the compressor fundamental frequency and higher harmonics reasonably well, as is shown in **Figure 14**.

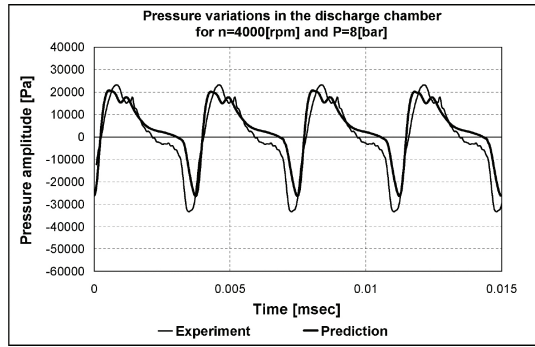


**Figure 13.** Gas pulsations calculated by coupled model, time domain.

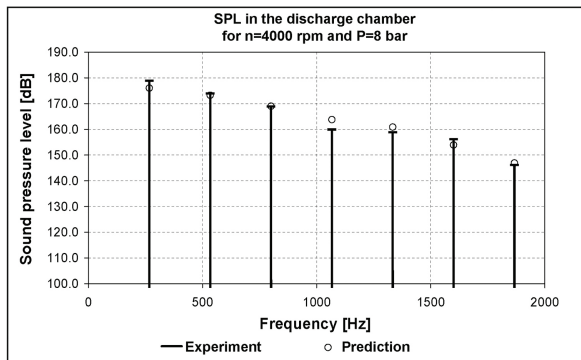


**Figure 14.** Gas pulsations calculated by coupled model, frequency domain.

Overall, the accuracy of the results calculated by the coupled model was considered to be sufficient to be used to analyse the influence of the compressor operational parameters and geometry upon the gas pulsations.

## 5. Parameters which influence gas pulsations

In order to reduce gas pulsation levels in the discharge chamber, the parameters which influence them have to be determined. Previous studies have reported the influence of some

of them, as well as on other aspects of compressor design and operation. However, there was no explanation why these parameters were selected from the many others possible. To investigate this and to find if there are any other significant parameters, previously overlooked, the discharge process was analysed.

### 5.1. Main factors which affect gas pulsations

The working and discharge chambers, connected through the discharge port, are presented in **Figure 15**. Both of these are also connected to the rest of the system outside of the compressor. The compressor working chamber is connected to the other working chambers, or to the suction chamber, through leakage paths, while the discharge chamber itself is connected to the discharge pipe. Connection between the chambers and their surroundings is always present. However, the connection between the working and discharge chambers is of a periodical nature. Accordingly, the discharge process of the working chamber starts with the opening of the discharge port and lasts only until the port is closed.

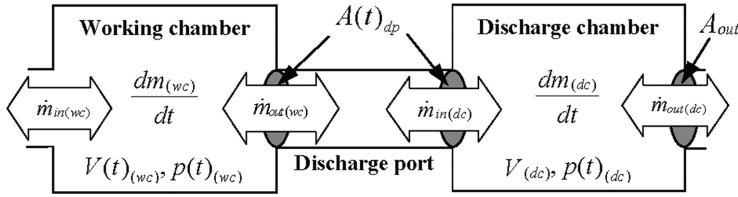


**Figure 15.** Screw compressor discharge system.

If the heat transfer through the chamber walls is neglected, then the gas condition in the chamber is determined by the change of the chamber volume and by the mass and energy transfer rates between the chamber and its surroundings. The volume of the working chamber is defined by the machine geometry and is expressed as a time-varying volume function, but the volume of the discharge chamber is constant. Therefore, it follows that the gas state in the discharge chamber is influenced only by the mass and energy transfer rates. This corresponds with the fact that gas pulsations in a chamber occur only if mass transfer rates to it are unsteady.

In **Figure 15**, two mass flows are shown between the discharge chamber and its surroundings. The first is the mass inflow into the discharge chamber from the compressor working chamber. The second is the mass outflow from the discharge chamber into the compressor discharge system consisting of pipes, oil separators and similar components. Both flows are time dependent and need to satisfy continuity Eqs. (3) and (4):

$$\dot{m}_{in(dc)} = \rho v A(t)_{dp} \quad (3)$$

$$\dot{m}_{ou(dc)} = \rho v A_{ou} \quad (4)$$

These equations show that both mass flows depend upon the instant gas density and the velocity. The fluid velocity is dependent upon the difference of fluid enthalpies in the chambers. For compressors, this is equivalent to the velocity being proportional to the square root of the pressure difference between the chambers. The gas density is also a parameter which is related to the chamber pressures. Therefore, the pressure difference between the working and discharge chambers is a parameter which influences the gas pulsation levels. Thus, the pressure difference between the discharge chamber and the pipe system is a result of the gas pulsations rather than their cause.

By analysing Eqs. (3) and (4), two more parameters can be identified which influence mass flow and later gas pulsations. The first is the outlet area,  $A_{\text{out}}$  where the discharge chamber is connected to the discharge pipe. This outlet area is constant and it is good to make it as large as possible. A larger area will cause less pressure difference for the same flow between the discharge chamber and pipe and will therefore stabilise the pressure in the discharge chamber.

The second parameter, which influences the mass flow, which has not been properly considered in previous studies, is the cross-sectional area between the working and discharge chambers,  $A(t)_{\text{dp}}$ , defined at the discharge port. According to Eq. (3), the effect of variation of the discharge port size is of the same order of magnitude as those of changes in density or velocity. This implies that the gas flow variation and pressure pulsation can be altered by modifying the discharge port area function. This can be achieved by changing the shape of the discharge port.

The influence of different discharge ports has been noticed but not explained in papers published by Errol and Ahmet [17] and Mujić et al. [18]. The difference in noise, identified through their research, can be explained only by the different cross-sectional area of the ports. The authors are not aware of any published results of investigations of this phenomenon.

It follows that the two basic parameters which influence the level of gas pulsations in the discharge chamber are the pressure difference and the discharge port area function. In order to reduce the amplitude of gas pulsations in the discharge chamber, these two parameters need to be optimised. It is necessary to explore and to optimise at least one of these two parameters.

The influence of the pressure difference has been explored in many studies. The most relevant are probably the papers from Koai and Soedel [5] and Sangfors [9]. They recognise pressure difference as a cause for gas pulsations and they have explored the influence of the compressor operational and design parameters upon the gas pulsations.

## 5.2 Parameters related to working conditions

Discharge pressure is a parameter which will determine the pressure difference between the working and discharge chambers at the moment when the discharge process starts. The pressure difference is the smallest when the discharge pressure is equal to the pressure in the working chamber. This has been reported by Koai and Soedel [4]. They noticed that the gas pulsations are a function of the discharge pressure and have a minimum. This is also confirmed later by Sangfors [6]. According to Huagen et al. [9], this minimum corresponds to the discharge pressure that matches the machine built-in volume ratio. Koai and Soedel [4] claim

that this minimum does not correspond exactly to that pressure, while Gavric and Badie-Cassagnet [19] considers that it occurs when there is small under-compression.

#### *5.2.1. Rotational speed*

Sangfors [6] and Huagen et al. [9] concluded that the amplitude of the pressure pulsations during the discharge process increases with the rotational speed.

#### *5.2.2. Oil influence*

Oil has an attenuating influence upon the noise generation process. According to Sangfors [6], this is significant at harmonics higher than the third order, but Tantari [8] states that this is noticeable only above the fifth order.

### **5.3. Compressor design parameters**

#### *5.3.1. Clearances*

Reduction of the leakage flow within the compressor, due to smaller clearances, increases the noise level generated in the discharge port. Soedel [4] and Sangfors [6] reported that for the same working conditions, changes of compressor clearances alter the working chamber pressure and fluid flow through the discharge port.

#### *5.3.2. Discharge chamber length*

According to Sangfors [6], the gas pulsations and generated sound pressure level (SPL) are affected by the length of the discharge chamber. This influence is significant and the sound pressure level, being a function of the chamber length, has a minimum for a certain chamber length.

### **5.4. Number of rotor lobes**

According to Sangfors [6], the number of rotor lobes influences the noise level. Rotors consisting of more lobes generally generate a lower sound pressure level in operation than those with fewer lobes.

All these parameters have a common factor in that they directly influence the pressure difference between the working and the discharge chambers. Operational parameters such as discharge pressure and compressor speed have a high influence on gas pulsations. However, those parameters depend on the purpose for which the compressor is used. This makes them inappropriate for optimisation. Compressor design parameters such as the built-in volume ratio, the clearances, the number of lobes and the sealing line length also affect gas pulsations. However, attempts to decrease gas pulsations by optimising any of these parameters, usually degrades the compressor performance and hence makes them unsuitable as parameters for optimisation.



Mujić et al. [10] showed how the time function of the discharge port affects gas pulsations in screw compressors. An example of varying the shape of the discharge port and its influence on gas pulsations will be presented here. For this purpose, models of the discharge process, already described, were used to determine the effect of the discharge port shape upon the level of gas pulsations. The other design parameters, such as the built-in volume ratio, clearances and sealing line length, were maintained constant. By this means any reduction in pulsations and change in efficiency can be attributed exclusively to the variation in port shape.

## 6. Gas pulsation reduction by use of discharge port alteration

Both experimental and numerical results were obtained for two different port shapes, to investigate their influence on the levels of gas pulsation in the discharge port. The numerical results, already given to evaluate the accuracy of the models, were used and will not be presented again. Instead, only the experimental results for different shapes of discharge port will be analysed.

### 6.1. Compressor testing range and instrumentation

For the purpose of this investigation an oil-flooded air screw compressor was used because it operates over a larger pressure range and develops higher gas pulsations than an oil-free compressor. In addition, an oil-injected screw compressor does not need synchronising gears, which affect the overall compressor noise level, and it may be driven at moderate speeds. Therefore, the noise generated by the test compressor was mainly caused by the gas pulsations. The compressor parameters are given in **Table 1**.

Compressor design parameters			Main	Gate
		Number of lobes	4	5
Centre distance	71 [mm]	Outer diameter	102 [mm]	80 [mm]
Rotor length	158 [mm]	Pitch diameter	63 [mm]	79 [mm]
Wrap angle	300 [deg]	Inner diameter	62 [mm]	40 [mm]
Pressure range	3–12 [bar]	Speed range	2000–6500 [rpm]	

**Table 1.** Screw compressor design parameters.

The test compressor was placed in a laboratory test rig, built to CAGI and PNEUROP standards. One set of measuring points covers the compressor speeds from 2000 to 6000 rpm at a discharge pressure of 8 bar, while the other set of points covers discharge pressures from 5 to 12 bar at a speed of 4000 rpm.

The discharge chamber pressure was measured by the use of an Endevco 8530C Piezoresistive pressure sensor to obtain a pressure function. The sound pressure level (SPL) around the test compressor was measured by pressure level indicators SJK. A sound Level Meter HML 323

was used to evaluate a correlation between the pressure function within the discharge chamber and the overall compressor noise. Measurements of the pressure, temperature, driving torque, air flow and compressor speed were also taken to estimate the compressor performance.

### 6.2. Modification of the discharge port

The original discharge port was modified to reduce the amplitudes of the gas pulsations by minimising any sudden flow between the working and discharge chambers at the beginning of the discharge process, when the pressure difference between the chambers is highest. According to Eq. (3), this flow is governed by the pressure difference and the size of the port area. Since the built-in volume ratio was not changed, the pressure difference was the same for both modified ports at the moment when discharge started. The original discharge port was designed to have the largest possible opening for any rotor position, in order to reduce flow losses. This was achieved by designing the port shape to correspond with the shape of the rotor trailing edges. Such an approach generates a discharge port area function with a high starting gradient, as shown by the light line in **Figure 16**. In that case the port has the largest opening when the pressure difference is largest.

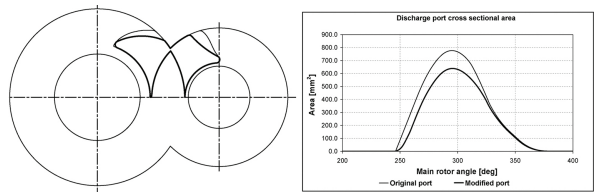


**Figure 16.** Shape and cross-sectional area of two different discharge ports.

To avoid this, a new port shape was devised, as shown by the bold line in **Figure 16**, where it can be seen clearly that only the port opening curves were changed. This altered the starting gradient of the port area function while maintaining the same built-in volume ratio as the original by keeping the remaining parts of the opening curves unchanged. Therefore, both ports opened at the same rotor position. The opening curves are simple in this second case and consist of only three arcs. They are therefore simpler than in the old port. The pressure function in the discharge chamber, predicted by the simulation models of the discharge process, showed a reduction in gas pulsations.

The shape modification of the port reduces the size of the port area. This difference increases at the beginning of opening and is highest when the port is fully open. It then decreases as the port closes and finally disappears when the leading edges of the following rotor lobes cover the opening curves of the port completely. Such a reduction must cause some flow losses.

### 6.3. Experimental verification of results

The shape of the compressor discharge port geometry, presented in **Figure 16**, was changed to verify the predicted results by locating metal inserts to form the new port. These inserts also

covered the original opening curves on both sides of the port. These are illustrated in **Figure 17** by the two lines on the metal inserts. After modification, a new set of measurements was carried out in order to compare with the predicted gas pulsations.

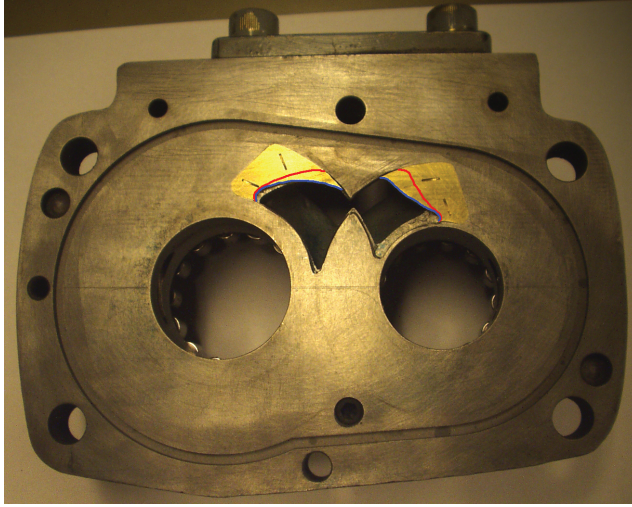


**Figure 17.** Modified shape of the discharge port.

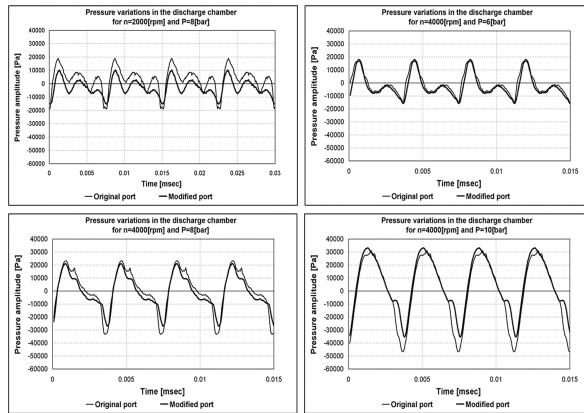


**Figure 18.** Comparison of experimental data for original and modified discharge ports.

The measured values of the pressure functions in the discharge chamber for the original and modified discharge ports are compared in **Figure 18**. These are shown for the original and modified port by light and bold lines, respectively. It can be seen that the gas pulsation amplitudes are reduced across the whole range of working conditions. As shown in **Fig-**

ure 19, the sound pressure level, generated by gas pulsations in the discharge chamber, is reduced.

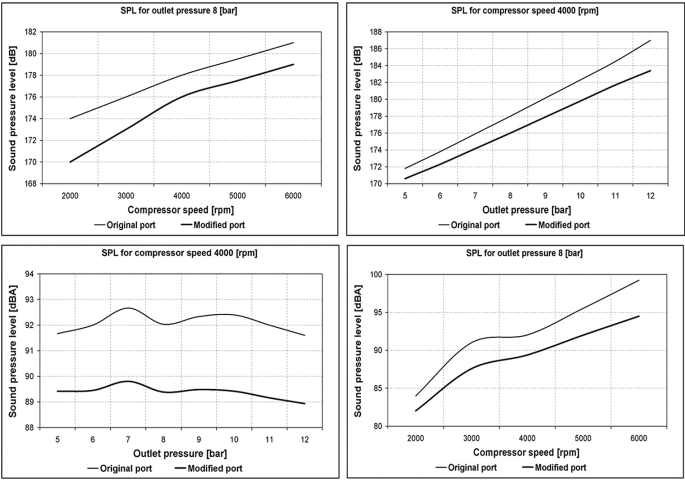


Figure 19. Comparison of calculated SPL inside the discharge chamber and measured SPL around compressor for original and modified discharge ports.

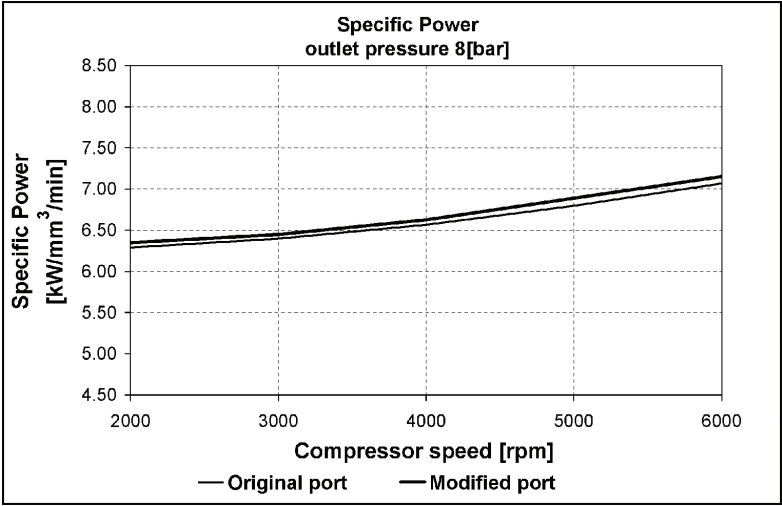
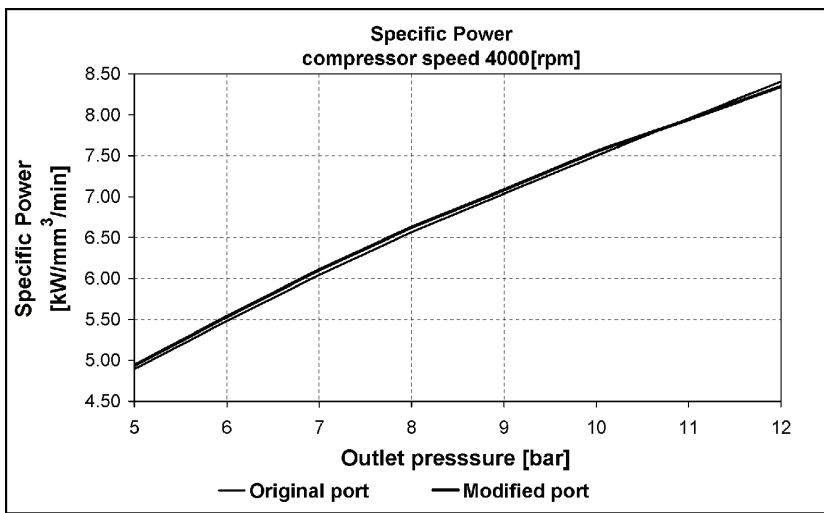


Figure 20. Compressor-specific power for different outlet pressures.

More specifically, as can be seen in Figure 19, the overall noise in the compressor environment is attenuated by about 3 dB at 4000 rpm over the whole pressure range, while there is a

noticeable noise reduction across the compressor speed range, varying from 2 dB at the lowest speed up to 5 dB at the maximum speed for an outlet pressure of 8 bar. The use of the model therefore represents a good step towards identifying the influential parameters and overall noise reduction

Since modification of the discharge port reduced the flow area, the flow losses were increased, thereby affecting the compressor performance. The compressor with the modified port requires more power than that with the original port and a comparison of the specific power for the two versions of the machine is presented in **Figures 20** and **21**. **Figure 20** shows that, over the whole speed range, the compressor with the modified port consumed more power at a constant outlet pressure of  $p_{\text{out}} = 8$  bar.



**Figure 21.** Compressor-specific power for different speeds.

A comparison of the specific power, presented in **Figure 21** for a compressor constant speed of 4000 rpm, shows that the compressor with the modified port consumes more power for the majority of the pressure range. However, for the highest pressures in the range, the specific power is lower for the new port. The reason for this is that the new port shape reduces back flow when the compressor operates at higher pressures.

## 7. Conclusion

Basic analysis has shown that the two most influential parameters affecting gas pulsations in a screw compressor discharge chamber are the pressure difference between the compressor working and discharge chambers and the discharge port area. Mathematical models applied to calculate the pressure function in a screw compressor discharge chamber have shown that

1 the gas pulsations in a screw compressor discharge port and, consequently, the generated noise  
 2 can be reduced by making appropriate changes to the shape of the discharge port. This has  
 3 been confirmed by good agreement obtained over a wide range of speeds and pressures  
 4 between predicted and measured values in a compressor with two different port shapes.

## 5 Acknowledgements

6 Majority of the material presented in this chapter is reproduced from PhD Thesis, "A Numerical  
 7 and Experimental Investigation of Pulsation Induced Noise in Screw Compressors", by  
 8 Mujić E, submitted at City University London in 2008, ref. [20].

## 9 Author details

10 Elvedin Mujić<sup>1\*</sup>, Ahmed Kovačević<sup>2</sup>, Nikola Stošić<sup>2</sup> and Ian K. Smith<sup>2</sup>

11 \*Address all correspondence to: elvedin.mujić@bitzer.de

12 1 BitzerKühlmaschinenbau GmbH, Sindelfingen, Germany

13 2 City University, London, United Kingdom

AQ1

## 14 References

- 15 [1] Stošić N, Mujić E, Kovačević A, Smith I K. Development of rotor profile for silent screw  
 16 compressor operation. In: International Conference on Compressors and their Systems  
 17 2007; London, UK. London, UK: IMechE; 2007. p. 133–145.
- 18 [2] Holmes C S. Transmission error in screw compressors, and methods of THEIR?  
 19 Compensation during rotor manufacture. In: International Conference on Compressors  
 20 and their Systems 2005; London, UK. London, UK: IMechE; 2005. p. additional paper.
- 21 [3] Fujiwara A, Sakurai N. Experimental analysis of Screw Compressor Noise and  
 22 Vibration. In: In The 1986 International Compressor Engineering Conference at Purdue;  
 23 West Lafayette, US. West Lafayette, US:1986.
- 24 [4] Koai K L, Soedel W. Gas pulsations in twin screw compressors – Part I: Determination  
 25 of port flow and interpretation of periodic volume source. In: The 1990 International  
 26 Compressor Engineering Conference at Purdue; West Lafayette, US. West Lafayette,  
 27 US: 1990. p. 369–377.
- 28 [5] Koai K L, Soedel W. Gas pulsations in twin screw compressors – Part II: Dynamics of  
 29 discharge system and its interaction with port flow. In: In The 1990 International

- Compressor Engineering Conference at Purdue; West Lafayette, US. West Lafayette, US: 1990. p. 378–387.
- [6] Sangfors B. Computer simulation of gas-flow noise from twin-screw compressors. In: International Conference on Compressor and Their Systems; London, UK. London, UK: IMechE; 1999. p. 707–716.
- [7] Sangfors B. Modelling, measurement and analysis of gas-flow generated noise from twin-screw compressors. In: The 2000 International Compressor Engineering Conference at Purdue; West Lafayette, US. West Lafayette, US: 2000. p. 971–978.
- [8] Tanttari J. On twin-screw compressor gas pulsation noise. In: The 29th International Congress and Exhibition on Noise Control Engineering; 27–30 August; Nice, France. 2000. p. 2369–2372.
- [9] Huagen W, Ziwen X, Xueyuan P, Pengcheng S. Simulation of discharge pressure pulsation within twin screw compressors. *Proceedings of the IMECH E Part A Journal of Power and Energy*. 2004;218(4):257–264.
- [10] Mujić E, Kovačević A, Stošić N, Smith I K. The influence of port shape on gas pulsations in screw compressor discharge chamber. *Proceedings of the IMechE, Part E: Journal of Process Mechanical Engineering*. 2008;222(E4):211–223.
- [11] Soedel W. *Sound and Vibration of Positive Displacement Compressors*. New York, US: Taylor Francis Group; 2006.
- [12] Stošić N, Smith I K, Kovačević A. *Screw Compressors: Mathematical Modelling and Performance Calculation*. Berlin/Heidelberg/New York: Springer; 2005.
- [13] Kovačević A, Stošić N, Smith I K. *Screw Compressors Three Dimensional Computational Fluid Dynamics and Solid Fluid Interaction*. Berlin/Heidelberg/New York: Springer; 2006.
- [14] Lee W S, Ma R H, Chen S L, Wu W F, Hsia H W. Numerical simulation and performance analysis of twin screw air compressor. *International Journal of Rotating Machinery*. 2001;7(1):65–78.
- [15] Kolade B, Morel T, Kong S C. Coupled 1-D/3-D analysis of fuel injection and diesel engine combustion. *Journal of Engines*. 2004;113.
- [16] Kovačević A, Mujić E, Stošić N, Smith I K. An integrated model for the performance calculation of screw machines. In: International Conference on Compressors and Their Systems; London, UK. London, UK: IMechE; 2007. p. 757–765.
- [17] Erol H, Ahmet G. The noise and vibration characteristics of reciprocating compressor: Effects of size and profile of discharge port. In: The 2000 International Compressor Engineering Conference at Purdue; West Lafayette, US. West Lafayette, US: 2000. p. 677–683.

1 [18] Mujić E, Kovačević A, Stošić N, Smith I K. Analysis and measurement of discharge port  
2 influence upon screw compressor noise. In: TMT 2005; Antalya, Turkey. 2005. p. 993–  
3 996.

4 [19] Gavric L, Badie-Cassagnet A. Measurement of gas pulsations in discharge and suction  
5 lines of refrigerant compressors. In: The 2000 International Compressor Engineering  
6 Conference at Purdue; West Lafayette, US. West Lafayette, US: 2000. p. 627–634.

7 [20] Mujić E. A Numerical and Experimental Investigation of Pulsation Induced Noise in  
8 Screw Compressors, PhD Thesis, City University London; 2008.

**AUTHOR QUERIES**

AQ1	Please provide department name in affiliations.
AQ2	Please check the hierarchy of the section headings.
AQ3	Please provide the page number in reference "15."
AQ4	Please provide significance for the designators "A, B, C, D" present in the artwork of Figure 1.
AQ5	Please check the layout of Table 1.